

RADIO ASTRONOMY &
THE GALACTIC ROTATION CURVE

Senior Thesis
Submitted: April 1, 2008

KELVIN L. VARGHESE
Bachelor of Science Candidate, May 2008

Southern Methodist University
Department of Physics

Abstract

A radio telescope is used to make spectral observations of neutral hydrogen in the Milky Way. The fundamentals of the radio telescope, the primary tool of radio astronomy, are explored. Analysis of the geometry in which the observations are made as well as use the Doppler shift formula allows for a plot of the rotation speed of the galaxy as a function of distance from the center of the galaxy. Historically, this galactic rotation curve is a significant result that provided early indications that the mass of the galaxy cannot be solely luminous matter.

Contents

1	Theory	3
1.1	HI Line	3
1.2	Expected Shape of the Rotation Curve	3
1.3	Measuring the Rotation Curve	5
2	Experimental Apparatus	7
2.1	Antenna	8
2.2	Receiver	9
2.3	Software	10
3	Procedure	10
4	Results	10
4.1	Empirical Study of the Rotation Curve	10
4.2	Experimental Rotation Curve	11
4.3	Discussion	12
5	Conclusion	14
A	Data Analysis	15

1 Theory

The galactic rotation curve is a plot of the radial velocity of the galaxy (rotating about the center of the galaxy) as function of distance from center of the galaxy. This plot is obtained by measuring the Doppler shift of the 21 cm spectral line for neutral hydrogen—the HI line—at various galactic longitudes l along the galactic equator (galactic latitude $b = 0^\circ$) [1, 154].

1.1 HI Line

Neutral hydrogen is a reliable source for this sort of measurement. It is the most common element in the interstellar medium—the mixture of gas, dust and high-energy particles between stars [1, 153]. At low temperatures, such as those in space, the only transitions that hydrogen undergoes correspond to changes in spin of the lone electron relative to the nucleus [2, 8-87]. During a hyperfine transition, the relative spin flips from parallel to anti-parallel (the energy of the parallel configuration is greater than that of the anti-parallel configuration) and a photon of wavelength 21 cm (or frequency 1420.4 MHz) in the radio range (detectable by a radio telescope) is emitted [4, 1] [2, 8-89] [8, 105]. Since the photon is of lower frequency than visible light, it is unimpeded by interstellar dust; this limitation to optical telescopes is avoided in radio telescopes [4, 1]. It was, in fact, studies of hydrogen distribution in the universe with radio astronomy that predicated the characterization of the Milky Way as a spiral galaxy (see Kerr and Westerhout (1964), et al.) [2, 8-88].

1.2 Expected Shape of the Rotation Curve

In a spiral galaxy, stars are in a circular orbit about the center of the galaxy ([6, 130-131] for the entirety of the following discussion). The acceleration a for an object in circular motion is described by

$$a(r) = \frac{v^2}{r}$$

where v is radial velocity and r is the radius of the orbit. If the only force acting on the star is gravitational attraction of the galaxy, then the acceleration a is further described by Newton's Law of Gravitation:

$$a(r) = G \frac{M(r)}{r^2}$$

where G is the gravitation constant and $M(r)$ is the mass within radius r . Equating the two descriptions and solving for velocity:

$$\begin{aligned} \frac{v^2}{r} &= G \frac{M(r)}{r^2} \\ v(r) &= \sqrt{G \frac{M(r)}{r}} \end{aligned}$$

Thus, the radial velocity is related to the radius by $v \propto \frac{1}{\sqrt{r}}$; this relation is known as Keplerian rotation [6, 131]. This relation is not appropriate, however, for all r because mass (considering only luminous matter), is not evenly distributed for all r . A spiral galaxy contains two components: a central disk and the spiral arms. Most of the mass is contained in the central disk; this assertion is justified by considering the surface brightness I of the central disk for a spiral galaxy:

$$I(r) = I_0 e^{-\left(\frac{r}{r_s}\right)}$$

where r_s is a scale length (for the Milky Way, $r_s \approx 4$ kpc) [6, 130]. The surface brightness decreases exponentially and thus, the mass of luminous matter can be approximated to behave similarly. The central disk can then be treated as a rotating solid body. The radial velocity in that case is simply

$$v(r) = r\omega(r)$$

where $\omega(r)$ is the angular velocity at r [7, 298]. Because the mass is concentrated at the center of the galaxy, at progressively larger radii, the mass will be constant. Thus, Keplerian rotation is appropriate for describing orbital velocity at large radii.

Based on this analysis, the rotation curve of the galaxy is expected to be linearly increasing for small r (the central disk) and decreasing as the inverse square root of r for larger r (the spiral arms) as shown below:

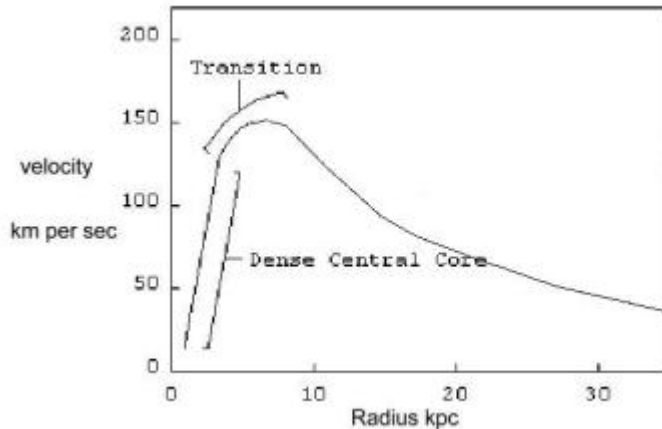


Figure 1: Central mass approximation model [?]

As experiments (see Burton & Gordon (1978), et al.) have shown, the actual curve is very much *unlike* the expected curve (for a further discussion of the results of empirical studies, see Section 4: Results below).

1.3 Measuring the Rotation Curve

Since the frequency of the 21 cm hydrogen line is known, measurements of the redshift at various galactic longitudes allow for the calculation of the velocity of the source using the equation describing Doppler shift at distances that can be calculated using geometry describing the motion of the sun relative to the galactic center. Then the galactic rotation curve is plotted with the calculated distances vs. calculated radial velocities. Note that “orbital velocity” and “radial velocity” are used interchangeably.

When measuring the frequency of hydrogen at various lines of sight in the universe, it is not expected that the frequency will be 1420.4 MHz since there is relative motion between the source and the observer. Its frequency, however, will be shifted in a well-defined manner known as the Doppler shift

$$\mp v = \frac{\pm \Delta \nu}{\nu} c$$

where v is the velocity of approach (–) or recession (+), c is the speed of light, $\Delta \nu$ is the frequency shift, and ν is the rest frequency (for HI, $\nu = 1420.4$ MHz) [2, 8-89].

For observations with galactic longitudes $0^\circ < l < 90^\circ$, the hydrogen is receding from the observer (see Kerr and Westerhout (1964) as cited in [2, 8-91]). Thus, the frequency of hydrogen is expected to be “redshifted”, that is, less than the rest frequency. The velocity v is relevant in the discussion below; however, it is incomplete and a necessary correction for the frame of reference will be added.

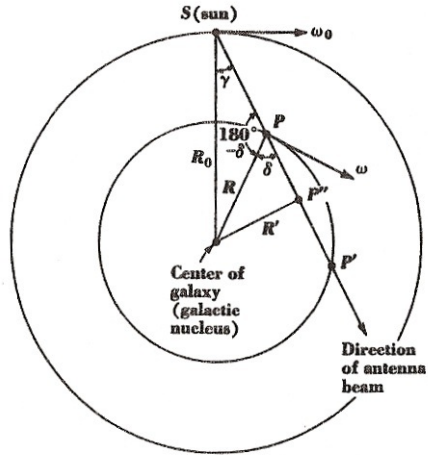


Figure 2: Simplified geometry of galactic motion [2, 8-92 (Fig. 8-62)]

Analyzing galactic motion requires an understanding of the relevant geom-

etry ([2, 8.92-8.8.93] for the entirety of the following discussion). Consider the figure above.

The point of interest (where measurement is intended) is the point P . The line of sight is labeled by “Direction of antenna beam”; naturally, the antenna beam intersects the point P . The antenna beam makes an angle γ with the galactic center; this angle is also the galactic longitude l . The velocity v of the point P relative to the point S (the sun) is described by

$$v = \omega R \sin \delta - \omega_0 R_0 \sin \gamma$$

where ω_0 is the angular velocity at the point S , R_0 is the radius of the point S from the galactic center, and δ is the angle at the point P between the antenna beam and the galactic center. The law of sines holds

$$\frac{\sin \gamma}{R} = \frac{\sin (180^\circ - \delta)}{R_0} = \frac{\sin \delta}{R_0}$$

which implies that

$$R \sin \delta = R_0 \sin \gamma$$

Replacing $R \sin \delta$ in the description of v yields

$$v = (\omega - \omega_0) R_0 \sin \gamma$$

For galactic longitudes $0^\circ < l < 90^\circ$, the maximum radial velocity occurs at the tangent point, where the line of sight is tangent to a circle centered on galactic center [4, 5]

$$R = R_0 \sin \gamma$$

Plugging this relation of R into the description of v yields

$$v = (\omega - \omega_0) R$$

The radial velocity V of the point P is generally

$$V = \omega R$$

and rearranging the description of v , it is apparent that

$$V = \omega R = v + \omega_0 R$$

Since the maximum radial velocity of the point P occurs at the tangent point R , the relation describing the rotation curve is

$$\boxed{V = v_{\text{max observed}} + \omega_0 R_0 \sin \gamma}$$

where V is the orbital velocity at a distance R from the galactic center, $v_{\text{max observed}}$ is the velocity corresponding to the maximum Doppler shift (a calculated quantity), $\omega_0 R_0$ is the orbital velocity the point S (which is taken to be the Sun, and thus, is a known quantity $\omega_0 R_0 = 220$ km/s), and γ is the galactic longitude (a known quantity) [4, 5] [9, 29-5].

This geometry is based on a simplified model referencing motion relative to the sun. Since both the motion of the sun and the motion of the observer on earth need to be considered, it is best to describe motion relative to the local standard of rest (LSR) [2, 8-93]. The LSR is defined as “the centroid of motion of the stars near the sun or local region of our home area of the galaxy” [2, 2-33]. Referring to motion relative the LSR allows for the removal of explicit reference to the earth’s motion about the sun and the sun’s drift with respect to the the centroid of motion [2, 2-33].

These considerations are manifest in the Doppler shift calculations. A full description of source velocity v is

$$v = \frac{\Delta\nu}{\nu}c - v_{\text{LSR}}$$

Then, for the maximum redshifted frequency,

$$v_{\text{max observed}} = \frac{\nu - \nu_{\text{max shift}}}{\nu}c - v_{\text{LSR}}$$

where ν is the rest frequency (for HI, $\nu = 1420.4$ MHz), $\nu_{\text{max shift}}$ is maximum redshifted frequency, and v_{LSR} is the velocity along the line of sight relative to the LSR [4, 2].

2 Experimental Apparatus

Spectral observations of the HI line along the galactic equator at various galactic longitudes are made by a radio telescope. The small radio telescope (SRT) used in this experiment is a prime focus reflector consisting of a 3.05 m diameter parabolic dish antenna with motorized two-axis azimuth/elevation mount enabling the telescope to point to and track specified locations in the sky. The telescope is fully computer controlled with a java application that that communicates with the controller, which controls the azimuth and elevation motors. The telescope receives information through a radio receiver mounted at the focus of the parabolic dish. The components of the SRT will be discussed in more detail below. The telescope is developed by Massachusetts Institute of Technology’s Haystack Observatory ([3] and [5] for entirety of the following section). The SRT used in this experiment is pictured below:



Figure 3: The SRT used in this research

2.1 Antenna

Since the sources of incident radio waves are far away, it is necessary that the telescope be designed to capture as much energy as possible. A parabolic antenna is optimal because it can place all the incident energy into a small spot where a feed, which communicates with a signal amplifier, can be placed [5, Sec. 5.3.1].

While the SRT is called “small”, it is generally larger than an optical telescope; this because the angular resolution—“angular area of the sky from which the telescope can collect emission”—is proportional to the wavelength of incident radiation divided by the diameter of the telescope [5, Sec. 3]. The wavelength range for visible light is $0.3 \mu\text{m}$ - $0.8 \mu\text{m}$ while the range for radio waves is 0.001 m - 30 m [5, Sec. 2.1]. Thus, in order for the radio telescope to achieve comparable resolution as the optical telescope, the radio telescope must be larger. Also, in general, the larger the antenna, the more energy of the incident radiation is captured [5, Sec. 5.3.1].

The antenna is constructed from mesh that will “reflect all incident microwave energy if the surface holes are less than 1/10th of the incident wavelength” [3, 2]. This prevents the measurement of extraneous electromagnetic radiation.

The beamwidth of the antenna—a range of angles over which the telescope

is sensitive for a particular wavelength—is usually given with the telescope sensitivity at half its maximum value [9, 29-4] [5, Sec. 5]. The full-width half maximum (FWHM) beamwidth θ_{FWHM} (in radians) is given by

$$\theta_{\text{FWHM}} = \frac{1.22\lambda}{D}$$

where D is the diameter and λ is the operating wavelength [5, Sec. 5.3.5, 6.2.3]. For the SRT, $D = 3.05$ m and for the HI line, $\lambda = 21$ cm. Thus, the beamwidth of the SRT antenna looking at the HI line is $\theta_{\text{FWHM}} = .08$ rad.

2.2 Receiver

The radio signal from the parabolic antenna is focused to an antenna feed horn. It passes through a 1420.4 MHz L-band probe and a low noise amplifier that provides 24 dB gain before arriving at the receiver [3, 3]. The receiver and feed horn are pictured below:



Figure 4: The receiver and feedhorn

The signal then passes through an image rejection mixer, which forms the product of two waveforms. The input and output of the mixer are related by

$$\cos \omega_1 t \cos \omega_2 t = \frac{1}{2} \cos (\omega_1 + \omega_2) + \frac{1}{2} \cos (\omega_1 - \omega_2)$$

The output goes through a band-pass filter with keeps the difference frequency and removes the sum frequency, as required for this application [3, 3]. After a few other filtering and amplifying elements, the frequency is converted to a voltage proportional to signal power by a “square-law” detector [3, 3]. Without the square-law detector the signal is represented by a voltage proportional to the

electric field as collected by the antenna; normally, it is more useful to measure signal power rather than the electric field [5, Sec. 6.3.1]. After passing through an integrator that produces a weighted time average, the signal is sent to the controller [5, Sec. 6.4.1].

The receiver is calibrated using a noise diode, which emits a known signal that is detected by the receiver [3, 3]

2.3 Software

The SRT is controlled through a java application that displays a detailed user interface including times, coordinates, antenna drive status, and a map of the sky, among other things. The SRT can be controlled actively in realtime by entering commands in the application itself or passively, by creating and running command files, which direct the SRT to move to and track a source, and then begin and end data collection. Also, particularly helpful is the fact that the software allows for the user to directly input galactic coordinates (in the command files), which are then converted to the azimuth and elevation coordinate system used by the motors.

3 Procedure

All data is gathered along the galactic equator (galactic latitude $b = 0^\circ$) at various galactic longitudes l in the range $0^\circ < l < 90^\circ$. Most of the objects in the Milky Way lie on the galactic equator. The SRT is directed via the software to point to a particular galactic coordinate (for example: $b = 0^\circ, l = 55^\circ$) and track the coordinate for a specified amount of time. During this time, the software writes the power received from the source to a data file. The data file contains the integrated power spectrum. Since only one galactic longitude is specified, there will be one data file per galactic longitude.

For this experiment, data is collected at longitudes at 5° intervals, beginning at $l = 5^\circ$ and ending at $l = 65^\circ$. This abridged range is selected to optimize the limited visibility resulting from the physical settings around the SRT. The data is collected at each coordinate for a duration between 1200 seconds and 1800 seconds. The antenna is centered on the rest frequency of the HI line $\nu = 1420.4$ MHz and the integrated power spectrum is divided into 64 bins around the rest frequency.

4 Results

4.1 Empirical Study of the Rotation Curve

Studies starting from the 1960's demonstrated that the rotation curve of the galaxy was substantively inconsistent with the expected curve. One such figure is below:

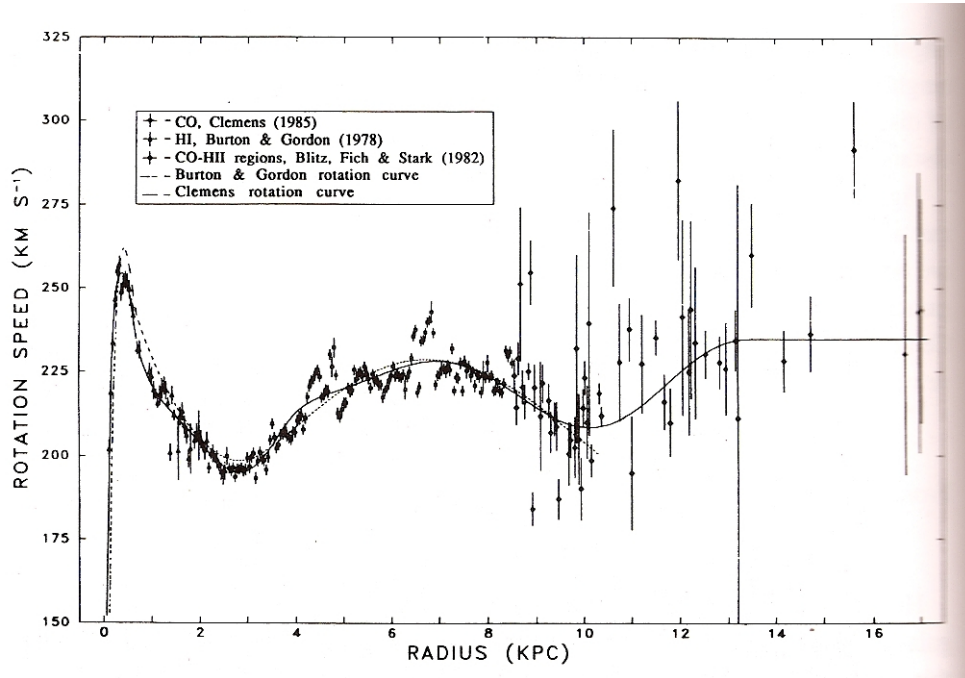


Figure 5: The rotation curve of the galaxy [1, 182, Fig. 10.4]

The velocity behaves linearly as expected for small R (the central disk portion of the galaxy). Unlike the expectation that the velocity would drop off like the inverse square root of the distance for larger R (the spiral arms), the data indicates that the speed stays roughly constant. The shape of the curve is more consistent with a mass distribution somewhere between a large central mass and uniform disk. The lack of decline in rotation speed indicates that our argument that most of the mass in the galaxy is concentrated at the center is wrong. But to the extent that this argument was based on observations of luminous matter, the mass difference is an indication that another source of mass is present in the galaxy. This additional mass was termed “dark matter” since study of luminous matter could not predict or verify its existence. The presence of dark matter seems to be strong beyond the central disk of the universe, providing enough mass in the spiral arms to prevent the rotation speed from declining.

4.2 Experimental Rotation Curve

Unfortunately, the results from this experiment do not resonate with previous studies. The rotation curve that resulted from the data collected is given below:

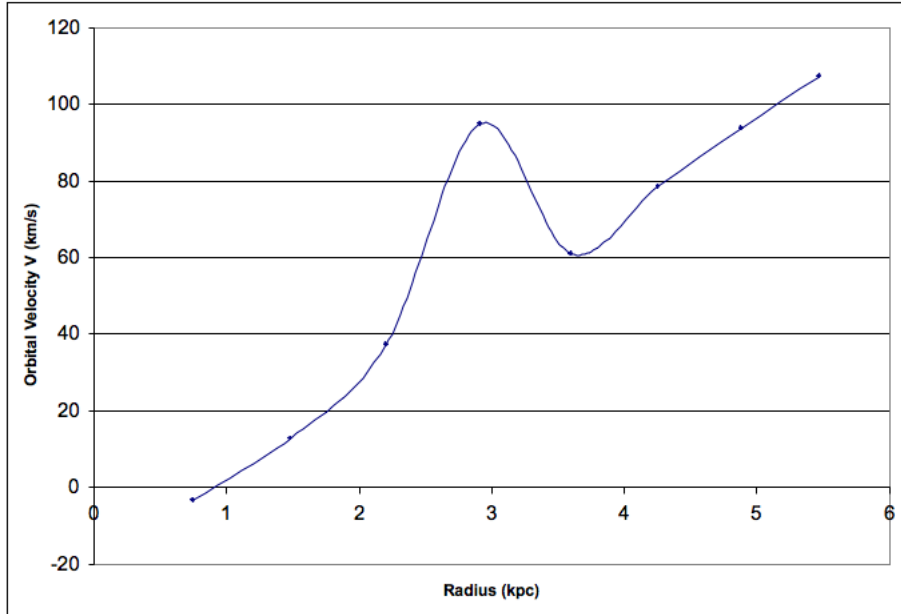


Figure 6: Rotation curve from this experiment

A more thorough explanation of the data analysis is given in Appendix A.

4.3 Discussion

On the one hand, one might take comfort in the fact that the experimental rotation curve does not exhibit inverse square root decrease in the rotation speed. In fact, the curve might suggest that the mass distribution of the galaxy is like solid disk for all R and one could argue that a significant amount of dark matter exists. But such comfort is unjustified. Consider the description of the rotation speed:

$$V = v_{\max \text{ observed}} + \omega_0 R_0 \sin \gamma$$

The $\omega_0 R_0 \sin \gamma$ piece is a linear relationship; there is no data at all involved in this piece. It is simply this linear relationship that is demonstrated in the experimental rotation curve. All of the meaningful data—that which provides the rotation curve with its shape—is contained in $v_{\max \text{ observed}}$. This piece is terribly deficient in this experiment.

There are any number of reasons for significant error in $v_{\max \text{ observed}}$. First, the beam of the antenna may not have been correctly aligned; this would result in the data being collected at a nominal coordinate which, in fact, was not the actual coordinate. The possibility of this source of error is apparent when

comparing an ideal scan (that is, a reference scan from a trusted source) of the Sun's brightness temperature versus the experimental scan.

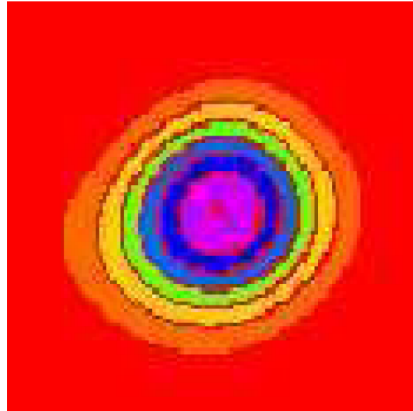


Figure 7: Ideal scan of the Sun's brightness temperature [3, 6, Fig. 6]

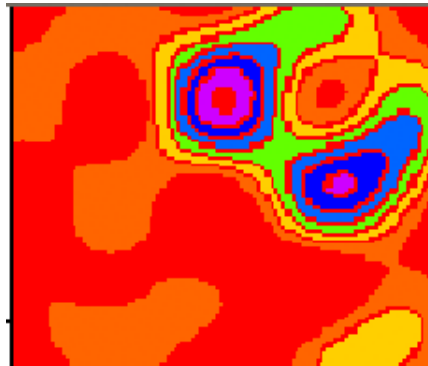


Figure 8: Experimental scan of the Sun's brightness temperature

A scan of the Sun's brightness temperature should be circular, as a Sun is, and centered in the window; the experimental scan is neither circular nor centered in the window. However, the experimental scan is not terribly unfocused: two areas of relatively high heat that are likely the inner part of the sun are apparent. The initial process by which the beam is aligned (as suggested in the operating guidelines) is slightly haphazardous, relying on the position of the shadow of the receiver.

Another source of error is the presence of blackbody radiation within the line of the sight of the telescope. This problem was noticed particularly at the

edges of the scan range where large trees stood. The power spectra near the blackbodies were an order of magnitude greater than other spectra.

The calibration of the receiver is completed using a noise diode; it is unclear whether the calibration is being properly conducted, which is another potential source of error.

During data analysis, it was noticed that for the relative velocity v calculation, using the adjusted Doppler shift formula, the adjustment portion v_{LSR} dominated the actual Doppler shift portion. This seems anomalous—the essence of this particular calculation is the redshift; with a massive v_{LSR} , the redshift is rendered meaningless. This anomaly raises the possibility that there is an issue with the v_{LSR} calculation in the software. This is particularly the case for $l > 50^\circ$. v_{LSR} was so dominant that the uncorrected spectrum (see Appendix A to distinguish between corrected and uncorrected velocity vs. power spectrum) demonstrated a *negative* baseline; because the meaning of these spectra was unresolved, they were excluded from the rotation curve.

5 Conclusion

While disappointingly the empirical galactic rotation curve was not recreated, this experiment facilitated a basic understanding of radio astronomy and the study thereof using radio telescopes. Also, in a mathematical sense at least, an understanding about one of the earliest indications of dark matter was formed.

A Data Analysis

Analysis of the data collected involves the following. The steps are discussed in limited detail.

1. A given data file, that is, the data collected at a particular galactic longitude is stored as an ASCII file (columns delimited by tabs/spaces) with the appendix .rad. The file may be opened in any data analysis tool; the research here used Microsoft® Excel®.
2. The file is opened and formatted. The columns of data are as follows (per the “Help” window in the SRT software):
 - field 1 - time (yyyy:ddd:hh:mm:ss)
 - field 2 - azimuth (deg)
 - field 3 - elevation (deg)
 - field 4 - azimuth offset (deg)
 - field 5 - elevation offset (deg)
 - field 6 - first frequency (MHz)
 - field 7 - digital frequency separation (MHz)
 - field 8 - digital mode
 - field 9 - number of frequencies in digital mode
 - field 10 - first frequency channel for digital receiver (K)
 - field 11 - second frequency (K)
 - following fields - continuation of frequency sequence (K)
 - last field - velocity of the local standard of rest v_{LSR} (km/s)
3. It is necessary to label each frequency channel by its respective frequency. In a new row below field 10 (the first frequency channel for the digital receiver) the value in field 6 (the first frequency) is inserted. The digital frequency separation is given by field 7; the remaining values of the new row (the frequencies) are filed in by adding the value of field 7 to the previous column. The end result is that each frequency channel is labeled by its respective frequency. The total numbers of channels (columns) is given by field 9.
4. The average v_{LSR} is found by averaging the values in the last field.
5. The frequency that is measured is the Doppler frequency; it is necessary to relate this Doppler frequency to the relative velocity along the line of sight v . The two are related by the usual description of Doppler shift

$$v = \frac{\nu - \nu'}{\nu} c - v_{\text{LSR}} = \frac{(1420.406 \text{ MHz} - \nu')}{1420.406 \text{ MHz}} - v_{\text{LSR}}$$

where v is the relative velocity of the source, ν is the rest frequency (for HI, $\nu = 1420.406$ MHz, ν' is the measured, redshifted frequency, c is the speed of light, and v_{LSR} is the velocity of the local standard of rest (a measured quantity). A new row with the calculated velocities is inserted.

6. A new row is created below the relative velocity v row with the value of the average power for each frequency channel.
7. Velocity versus average power is graphed. Notice that there is a positive, linear baseline as shown below (this is a graph of $b = 0^\circ$, $l = 55^\circ$):

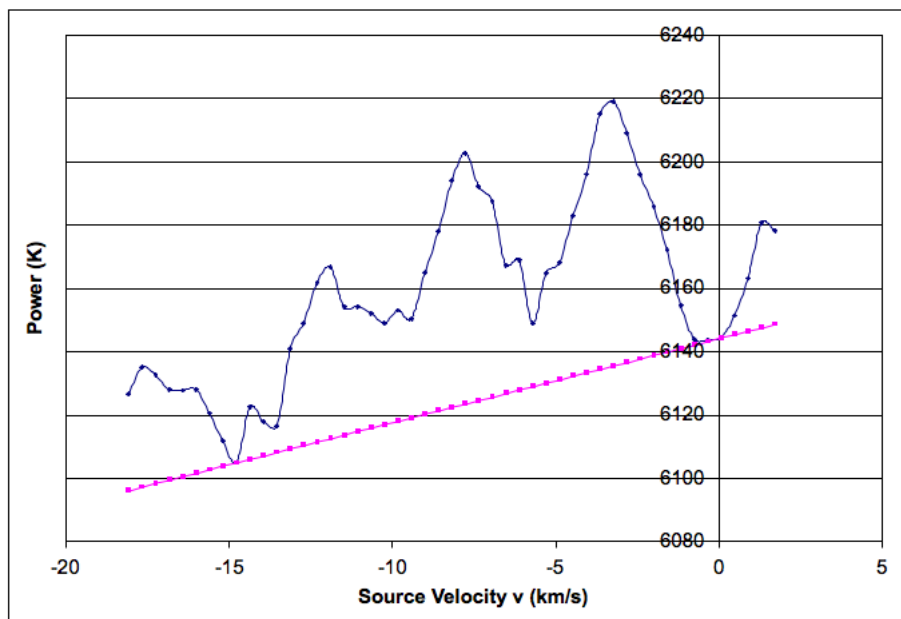


Figure 9: Uncorrected relative velocity versus power with baseline

8. A corrected row of average power is created by subtracting the baseline from the average power. The corrected plot (for the same coordinate) looks like this:

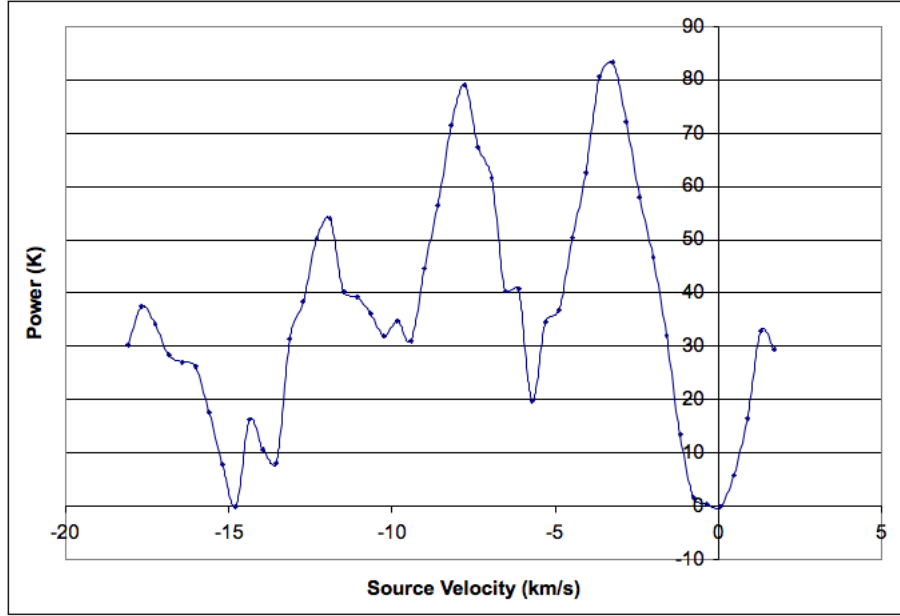


Figure 10: Corrected relative velocity versus power

9. The velocity corresponding to the maximum redshifted frequency $v_{\max \text{ observed}}$ is identified by locating the maximum non-zero velocity. In the graph above, $v_{\max \text{ observed}} = -1.178 \text{ km/s}$.
10. This procedure is repeated for every data file; $v_{\max \text{ observed}}$ is noted for each.
11. With the values of $v_{\max \text{ observed}}$ and the galactic longitude γ for each data file, $R = R_0 \sin \gamma$ and V can be calculated. Finally, the rotation curve is plotted based on the description:

$$V = v_{\max \text{ observed}} + \omega_0 R_0 \sin \gamma$$

References

- [1] Burke, Bernard F., Graham-Smith, Francis, *An Introduction to Radio Astronomy*, 2nd ed., Cambridge UP, Cambridge, 2002.
- [2] Kraus, John D., *Radio Astronomy*, 2nd ed., Cygnus-Quasar Books, Durham, NH, 1986.
- [3] MIT Department of Physics, *21-cm Radio Astrophysics*, web.mit.edu/8.13/JLEperiments/JLExp_46.pdf, December 2004.
- [4] MIT Haystack Observatory, *Measurement of Galactic Rotation Curve*, www.haystack.mit.edu/edu/undergrad/srt/SRT%20Projects/rotate.pdf.
- [5] MIT Haystack Observatory, *Radio Astronomy Tutorial*, www.haystack.edu/edu/undergrad/materials/RA_tutorial.html.
- [6] Ryden, Barbara, *Introduction to Cosmology*, Addison-Wesley, San Francisco, CA, 2003.
- [7] Serway, Raymond A., Jewett, Jr., John W., *Physics for Scientists and Engineers*, Vol. 2, 6th ed., Thomson-BrookCole, Belmont, CA, 2004.
- [8] Steinberg, J.L., Lequex, J., *Radio Astronomy*, McGraw-Hill, New York, NY, 1963.
- [9] University of Sydney School of Physics, *Experiment 29: Galactic Dynamics*, www.physics.usyd.edu.au/pdfs/current/sphys/3yr_lab/Expt_29.pdf, July 2007.